A Body-Blockage Analysis and Comparison Between Humans and a Full-Body Phantom

Using Measurements at 28 GHz

Khajeim, Maryam Faizi; Moradi, Gholamreza; Shirazi, Reza Sarraf; Zhang, Shuai

Published in:
I E E E Antennas and Propagation Magazine

DOI (link to publication from Publisher):
10.1109/MAP.2021.3089988

Publication date:
2022

Document Version
Accepted author manuscript, peer reviewed version

Body Blockage Analysis and Comparison between Human and Full-body Phantom Using Measurements at 28 GHz

Maryam Faizi Khajeim, Gholamreza Moradi, *Senior Member*, *IEEE,* Reza Sarraf Shirazi, Shuai Zhang, *Senior Member*, *IEEE*

***Abstract*—The human blockage is an important phenomenon that should be considered in millimeter-wave (mm-wave) communication systems. Realizing the blockage behavior could be very valuable in mm-wave link simulations. Several blockage models have been proposed in previous works based on knife edge diffraction (KED), high frequency simulations, and measurements. This work investigates the blockage using a full-body phantom and proves that the body phantom is accurate enough to replace the human subject in blockage studies for both data and talk modes. A campaign of measurements for these two modes with 17 human subjects of different heights and genders is conducted. The effect of different types of clothes on the body blockage is studied for body phantom and human subject. The impact of relative antenna-user position on the body blockage intensity is investigated, which is hard to do such accurate measurements with human subjects.**

***Index Terms*—5G, body blockage, body phantom, millimeter-wave, mobile terminal antenna, phased array, shadowing.**

I. Introduction

THE millimeter-wave (mm-wave) 5G systems have attracted enormous interest over the last ten years. The mm-wave is one of the key 5G technologies that can provide the high channel capacity required for new applications. Human blockage is one of the most important issues that should be considered in mm-wave bands. The mm-wave frequencies are more sensitive to human blockage than frequencies below 6 GHz. The human in the transmitter-receiver path can attenuate the signal significantly. The position of the human relative to the transmitter and receiver determines the human blockage intensity. Employing high gain directional antennas with beam scanning capability can considerably reduce the human blockage intensity [1]–[7].

Several investigations have estimated human blockage loss. The Third Generation Partnership Project (3GPP) TR38.901 [8] has proposed a rectangular region for the blockage area for both portrait and landscape modes. The blockage attenuation inside and outside the region is 30 dB and 0 dB, respectively. The Mobile and wireless communications Enablers for the Twenty-twenty Information Society (METIS) project has modeled the blockage based on knife edge diffraction (KED) [9]. In this model, each blocking object is approximated by a rectangular screen. The corresponding shadowing loss is modeled using a simple KED model for all four edges of the screen. A statistical blockage modeling using a 28 GHz form-factor prototype is proposed in [10], and in comparison with previous reports, a lower blockage loss of 5–20 dB is reported. A stochastic user shadowing model based on measurements with 18 subjects is presented in [11]. The impact of human body shadowing on the 60 GHz wideband channel is studied in [12]. The results of measurements are compared with the KED and the uniform theory of diffraction (UTD) based models.

The user impact on the circular polarized phased arrays for the 5G mobile terminal using the total scan pattern and coverage efficiency of the circular polarization is investigated in [13]. In [14], guidelines for optimum placement of a four-element phased array inside a 5G mobile phone are proposed using simulations and measurements for talk mode, data mode, and dual-hand mode. A statistical investigation on the user impact on the mobile terminal at 28 GHz by performing measurements with 12 human subjects for data and talk modes using body loss, coverage efficiency, and power in the shadow is presented in [15]. The user impact on the phased array in the mobile device at 15 GHz using human blockage measurements is studied in [16], and a body loss of 20–25 dB in the shadowing region is reported.

3GPP 5G specification (Release 15) has allocated four frequency bands between 24.25 GHz and 40 GHz for 5G new radio [17]. In this work, the blockage patterns of humans and the mm-wave full-body phantom (mmW-POPEYE10, SPEAG, Switzerland) [18] have been studied at 28 GHz. The phantom is unique with invariable height. Since the phantom will be used as a representative sample, it is valuable to study the impact of the user's height on the blockage pattern shape and power distribution. The results confirm that for people with torso height close to the phantom's torso height, the blockage patterns

Manuscript received October 21, 2020; revised June 9, 2020; accepted July 7, 2020. Date of publication November 1, 2020; date of current version April 16, 2019. (Corresponding author: Gholamreza Moradi).

M. Faizi Khajeim, G. Moradi, and R. Sarraf Shirazi are with the Microwave Measurement Research Laboratory, Department of Electrical Engineering, Amirkabir University of Technology (Tehran Polytechnic), Iran, Tehran 15875-4413 (e-mail: mfaizi@aut.ac.ir; ghmoradi@aut.ac.ir; sarraf@aut.ac.ir).

S. Zhang is with the Department of Electronic Systems, Aalborg University, 9220 Aalborg, Denmark (e-mail: sz@es.aau.dk).

are very similar. In some countries, the average height is shorter than the height of the phantom. Therefore, it would be beneficial to study a group of people with different torso heights. People usually are wearing clothes when they are using their mobile phones. The phantom is naked without clothes. It is necessary to study the effect of the clothes on the blockage pattern of the body.

The user's blockage pattern is compared with the free space radiation pattern of the user equipment (UE) antenna. The cumulative distribution function (CDF) of the blockage pattern and the correlation coefficient of patterns are used to study and compare different samples. The area of study in the φ direction is defined using different window sizes, which is shown in Fig. 3. The performed investigations show that the mm-wave phantom blockage is highly correlated with human subject blockage. That is a valuable conclusion because it confirms that the mm-wave phantom could be used for accurate and repeatable over-the-air (OTA) measurements of mobile phones instead of a human subject.

The contributions and novelties of this work are as follows.

- The performance of the full-body phantom is confirmed by comparing the phantom's blockage pattern with a group of human subjects with a height close to the phantom's height.
- The blockage pattern for a group of human subjects with a big difference in torso height with phantom has been studied.
- The impact of different types of clothes on the body blockage pattern has been studied.
- The effects of the relative distance, vertical position, and angle between mobile antenna and user have been investigated.

This paper is organized as follows. The measurement setup is explained in Section II. The blockage patterns of the phantom and human subjects are studied and compared for data and talk modes in Sections III and IV, respectively. In section V, the impact of different types of clothes on the body blockage is investigated. A blockage study for various scenarios using mm-wave phantom is presented in Section VI. Finally, a conclusion is given in Section VII.

II. Measurement Setup

A. UE Antenna

The antenna presented in [19] is used as the UE antenna, which is an 8×1 horizontally polarized antenna with an operating frequency band of 25 to 33 GHz. The antenna is placed in the bottom edge of the UE in the data mode and has an end-fire radiation pattern with a main beam toward the user. The user's hand does not touch the antenna; therefore, different hand grips do not affect the results significantly. Fig. 1 shows the antenna placement in the mobile phone with respect to the user in the data mode.

B. Millimeter-wave Phantom

The mmW-POPEYE10, which is a modular full-body phantom, is used in the blockage assessment measurements.

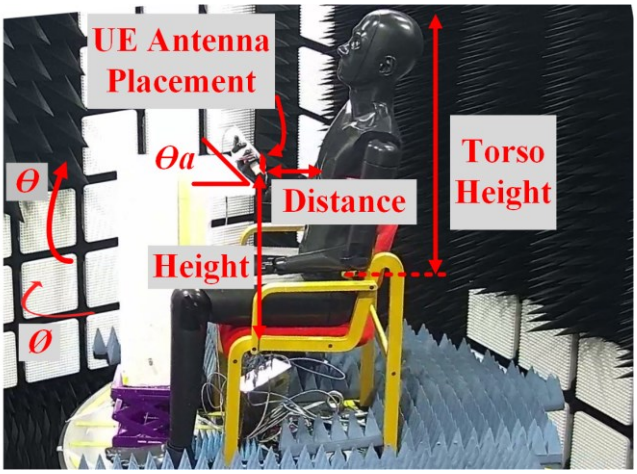

(a)

(b)

Fig. 1. The data mode measurement setup for (a) mmW-POPEYE10, (b) human subject.

The phantom is made of a lossy silicone-carbon-based mixture with material properties analogous to Cellular Telecommunications and Internet Association (CTIA) definitions for hand phantoms. A conductive skeleton is used to make a connection throughout the full-phantom, and a special low-loss silicone coating is employed that makes it efficient in the frequency range of 3-110 GHz. The fully posable structure enables the phantom to make the desired posture. The width, depth, and height of the phantom are 55, 30, and 185 cm, respectively [18].

C. Anechoic Chamber

The measurements were performed in the anechoic chamber at Aalborg University. The receiver antenna is a broadband horn antenna with a gain of 19 dBi at 28 GHz working from 18 to 40 GHz with a half-power beamwidth of 30˚. A calibration procedure is performed to remove the loss of cables and path. The measurement setup is shown in Fig. 1. A wooden chair with a small back fully covered by the user's torso is placed on a platform at the center of the anechoic chamber. The UE relative

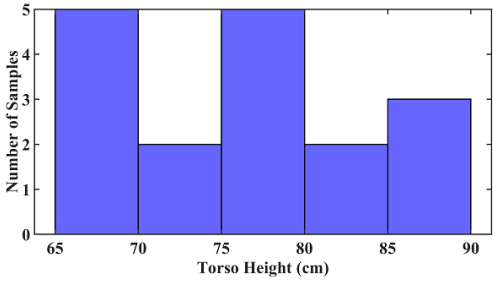

Fig. 2. The torso height distribution of human subjects.

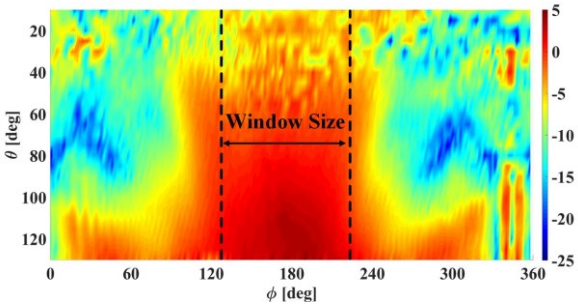

Fig. 3. The antenna free space radiation pattern.

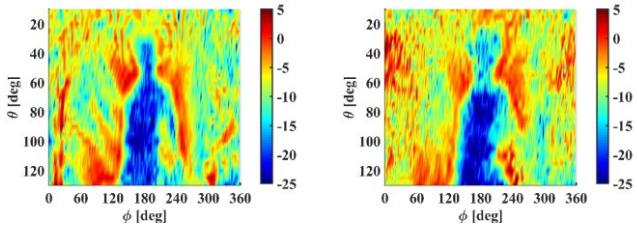

(a) (b)

Fig. 4. The blockage pattern of (a) phantom with torso height of 81 cm, and (b) human subject with torso height of 84 cm.

position to the body in the data mode is stabilized using a foam stand.

The probe on a robot arm scans with a step of 5˚ in the elevation plane, while the platform rotates in the azimuth plane with a step of 2˚. Since in the data mode, the blockage is mainly in the areas with a theta of 10˚ to 130˚. The measurement area in elevation is limited to 10˚ to 130˚ to decrease the measurement time to 30 minutes.

III. Data Mode Analysis

Fig. 1 illustrates the data mode measurement setup for the phantom and the human subject. In this posture, the body can be regarded as a scatterer on the path of the antenna main beam. The antenna position relative to the body is adjusted for a common single hand data mode posture. As illustrated, both phantom and human have the same posture in the data mode. The antenna-user distance and antenna's height above the chair seat are 17 cm and 43 cm, respectively. The angle of the antenna relative to the horizon (θa) is 45˚.

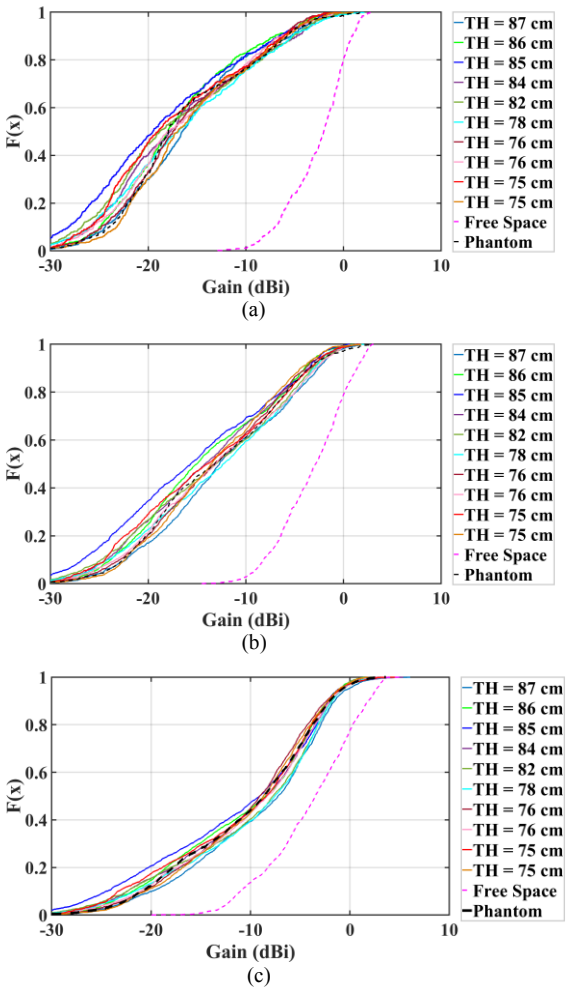

Fig. 5. The comparison of CDFs for phantom and group 1 subjects within a window size of (a) 40°, (b) 80°, and (c) 140˚.

A campaign of measurements with 17 human subjects, including 11 male and 6 female subjects is conducted. Depending on the antenna type, 8–13 test persons are required to provide reliable statistical data of the mean body loss [20]. The torso height distribution of human subjects is illustrated in Fig. 2.

Fig. 3 demonstrates the antenna free space radiation pattern. The blockage pattern of the phantom and a human subject is illustrated in Fig. 4. The torso height of the phantom and the human subject is 81 and 84 cm, respectively.

The subjects are separated into two groups: group 1 including 10 subjects having a maximum of 6 cm difference, and group 2 including 7 subjects having a 10 to 15 cm difference in torso height with the body phantom. Fig. 5 demonstrates the CDFs of the blockage pattern gain of the phantom and group 1 subjects within different window sizes. Window size indicates the studied area in the φ direction at the center of the shadow region.

The blockage pattern CDF is given as

$$F(X) = \frac{\iint 1\,(G\,(\theta,\phi) \le X)\; d\theta\; d\phi}{\iint\; d\theta\; d\phi} \qquad (1)$$

where 1 (•) is the indicator function and $G(\theta, \phi)$ is the blockage pattern gain of the spatial point (θ, ϕ). θ_{min} and θ_{max} are 10˚ and 130˚, respectively. ϕ_{min} and ϕ_{max} are defined as

$$\phi_{min} = 180° - window\ size/2$$
$$\phi_{max} = 180° + window\ size/2$$

The studies are performed within window sizes of 40°, 80°, and 140°. Window sizes of 40°, 80° are used to study the shadow region, and the window size of 140° includes the antenna coverage area, where the antenna radiation pattern is meaningful. The realized gain at the vertical edges of the window is around –6 dBi. It is observed that for group 1, at CDF of 0.6, the maximum difference between the blockage pattern gain of the phantom and human is 1.7 dB, 2.6 dB, and 1.2 dB within window sizes of 40°, 80°, and 140°, respectively. At CDF of 0.5, the maximum gain difference is 3 dB, 3.3 dB, and 2 dB within window sizes of 40°, 80°, and 140°, respectively.

The realized gain difference within all window sizes is less than 2.6 dB. It can be concluded that the blockage power distribution of the phantom and the subjects in group 1 are very close to each other. For the whole space, the CDFs of human subjects are very similar. The maximum gain difference between samples at CDF of 0.6 is 1.2 dB.

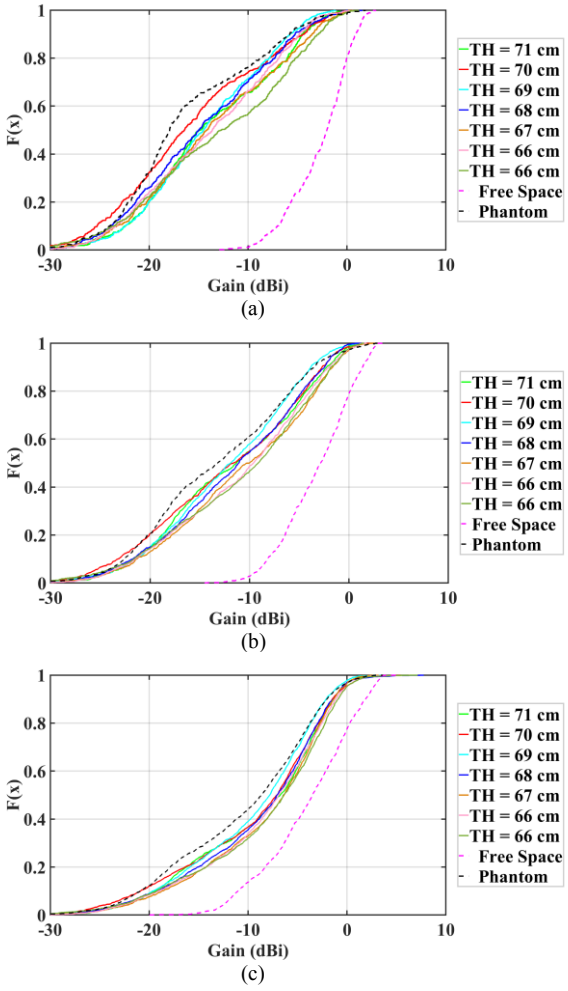

Fig. 6. The comparison of CDFs for phantom and group 2 subjects within a window size of (a) 40°, (b) 80°, and (c) 140˚.

Fig. 6 shows the CDFs of blockage patterns of phantom and group 2 subjects within different window sizes. It is observed that the blockage of the phantom is higher than that of human subjects within all window sizes. The maximum gain difference between blockage patterns of humans at CDF of 0.6 is 5.2, 2.4, and 1.5 dB within window sizes of 40°, 80°, and 140°, respectively. For the whole space, at CDF of 0.6, the maximum gain difference between phantom and humans is 2.2 dB.

The dimension of the user as a blocking object affects the power distribution in the shadow region considerably. As the height of the user decreases, more power can reach the area behind the user. Therefore, the height of the shadow region decreases. The torso height of the samples in group 2 is 10 to 15 cm shorter than that of the phantom. Therefore, it is expected to observe lower blockage for samples of group 2 than that for phantom and group 1. The results show that the smallest blockage is observed for the shortest sample with a torso height of 66 cm. At CDF of 0.6, the realized gain corresponding to the shortest human subject is 7.4 dB smaller than that of the phantom in the shadow region (window size of 40°).

The linear correlation coefficient is used to measure the association between blockage patterns of human subjects and phantom, which is given as

$$corcoeff = \frac{\sum_i (GH_i - \overline{GH})(GP_i - \overline{GP})}{\sqrt{\sum_i (GH_i - \overline{GH})^2}\sqrt{\sum_i (GP_i - \overline{GP})^2}} \quad (2)$$

where, GH and GP denote the human and phantom blockage pattern gains, respectively. $\overline{GH}$ and $\overline{GP}$ are the mean of GH and GP, respectively. The correlation coefficient lies between –1 and 1. It is completely positive correlated when it takes on a value of 1. It means that both considering variables increase together. If it takes on a value of –1, the variables would be

TABLE I
THE CORRELATION COEFFICIENTS OF THE PHANTOM* AND HUMAN SUBJECT'S BLOCKAGE PATTERNS IN THE DATA MODE

Group 1*				Group 2*			
Window Size / Torso Height(cm)	40°	80°	140°	Window Size / Torso Height(cm)	40°	80°	140°
87	0.8	0.8	0.68	71	0.72	0.62	0.59
86	0.72	0.73	0.59	70	0.7	0.68	0.6
85	0.78	0.72	0.62	69	0.65	0.63	0.58
84	0.78	0.77	0.65	68	0.64	0.61	0.53
82	0.8	0.77	0.67	67	0.51	0.55	0.48
78	0.78	0.78	0.65	66	0.51	0.45	0.43
76	0.77	0.71	0.58	66	0.55	0.47	0.47
76	0.78	0.78	0.67	–	–	–	–
75	0.76	0.72	0.6	–	–	–	–
75	0.77	0.71	0.6	–	–	–	–
Average	0.77	0.75	0.63	Average	0.61	0.57	0.53

* The torso height of the phantom is 81 cm.
* Group 1 includes subjects with torso height range of 75 to 87 cm.
* Group 2 includes subjects with torso height range of 66 to 71 cm.

completely negative correlated. The value of zero indicates that GH and GP variables are uncorrelated [21].

The correlation coefficients of blockage patterns of the phantom and human subjects are presented in Table I. Due to the short wavelength in the mm-wave band, a small movement of human subjects can affect the phase of the blockage pattern significantly. Therefore, the phase of the blockage pattern has not been considered in the correlation coefficient. It is observed that as the window size increases, the correlation between radiation patterns of different subjects with phantom decreases. It is due to random diffractions and reflections around the body. Beyond the shadow region, the scattering by the body affects the correlation coefficient considerably. Finer details of the structure of the body seriously affect the scattering of electromagnetic radiation by the body. Moreover, the skin type and clothes affect the electric field induced on the body. Therefore, the correlation between blockage patterns of different subjects with different dimensions, skin types, and clothes would be lower in the area beyond the shadow region.

IV. Talk Mode Analysis

The talk mode measurement setup is demonstrated in Fig. 7. The measurement setup is the same as the data mode setup. The antenna is positioned at a distance of 1 cm from the user's head and a relative angle of 25˚ to the horizon. In the talk mode measurements, two top edge-mounted and bottom edge-mounted modes are studied.

In the talk mode analysis like the data mode, the subjects are separated into two groups: group 1 including 10 subjects having a maximum difference of 6 cm, and group 2 having a 10 to 15 cm difference in torso height with the body phantom.

A. Top Edge-mounted Mode

The blockage patterns of the phantom and the human subject for the top edge-mounted mode are illustrated in Fig. 8. The torso height of the phantom and the human subject is 81 cm. Fig. 9 demonstrates the CDFs of the blockage patterns of the phantom and human subjects. At CDF of 0.6, a maximum difference of 4.2 dB and 5.1 dB between blockage patterns gain of the phantom and human is observed for group 1 and group 2, respectively. The maximum gain difference for group 1 at CDF of 0.6 is 7.4 dB between subjects with torso height of 86 cm and 87 cm.

The blockage patterns of the phantom and the human subject for the bottom edge-mounted mode are illustrated in Fig. 10. The CDFs of the blockage patterns of the phantom and human subjects are shown in Fig. 11. At CDF of 0.6, a maximum difference of 3.1 dB and 4.1 dB between blockage patterns gain of the phantom and human is observed for group 1 and group 2, respectively.

It can be concluded that there is no direct relation between power distribution and torso height in the talk mode. The antenna is close to the head, and the strength of the fields is highly dependent on the relative antenna-head position and interactions between them. Moreover, skin type, hair, head dimension, and glasses affect the scattering of electromagnetic waves by the user's head considerably. The correlation coefficients of blockage patterns of the phantom and human subjects in the talk mode are presented in Table II. In the talk mode for both top and bottom edge-mounted modes, the correlation coefficient is high for both groups. It can be concluded that the shapes of the blockage pattern are very similar for both modes and both groups. Since in the top edge-mounted mode, the antenna is closer to the head than in the bottom edge-mounted mode, the field strength

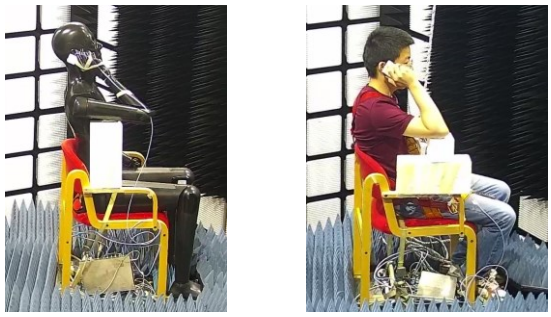

(a) (b)

Fig. 7. The talk mode measurement setup for (a) phantom, (b) human subject.

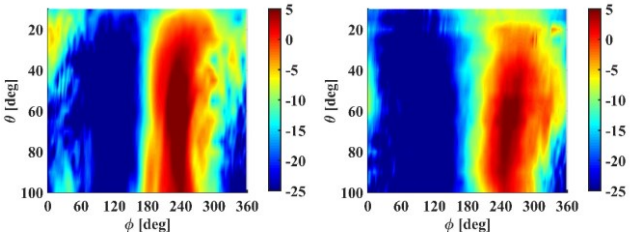

(a) (b)

Fig. 8. The blockage pattern for (a) phantom and (b) human subject with torso height of 81 cm in the talk top edge-mounted mode.

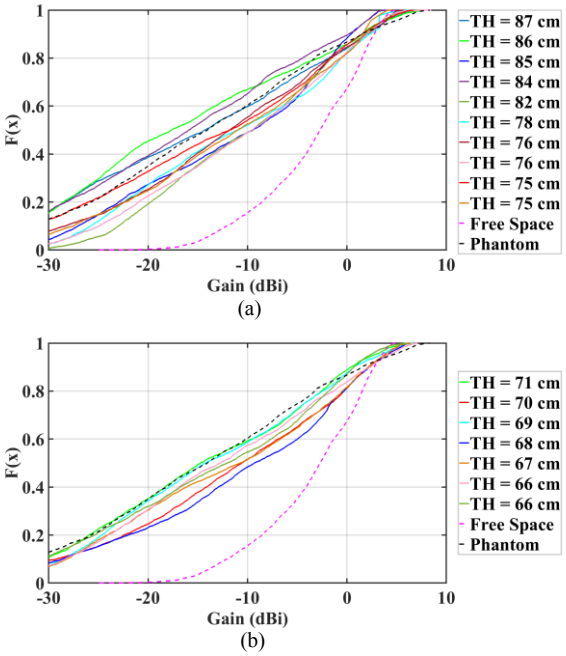

Fig. 9. The comparison of CDFs in the talk top edge-mounted mode for phantom and human subjects of (a) group 1, (b) group 2.

TABLE II
THE CORRELATION COEFFICIENTS OF THE PHANTOM AND HUMAN SUBJECT'S BLOCKAGE PATTERNS IN THE TALK MODE

Top Edge-mounted				Bottom Edge-mounted			
Group 1		Group 2		Group 1		Group 2	
Torso Height (cm)	Corcoeff	Torso Height (cm)	Corcoeff	Torso Height (cm)	Corcoeff	Torso Height (cm)	Corcoeff
87	0.83	71	0.88	87	0.79	71	0.75
86	0.77	70	0.8	86	0.85	70	0.77
85	0.82	69	0.81	85	0.7	69	0.8
84	0.85	68	0.7	84	0.78	68	0.8
82	0.82	67	0.88	82	0.7	67	0.75
78	0.8	66	0.71	78	0.8	66	0.75
76	0.87	66	0.82	76	0.8	66	0.78
76	0.81	–	–	76	0.79	–	–
75	0.77	–	–	75	0.83	–	–
75	0.75	–	–	75	0.79	–	–
Average	0.8	Average	0.8	Average	0.78	Average	0.77

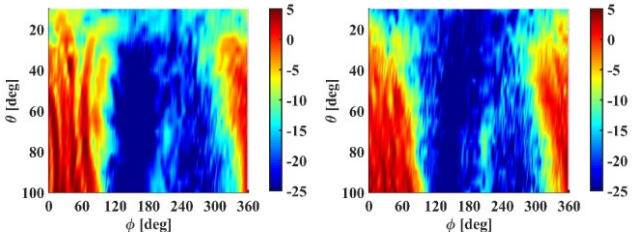

(a) (b)

Fig. 10. The blockage pattern for (a) phantom and (b) human subject with torso height of 81 cm in the talk bottom edge-mounted mode.

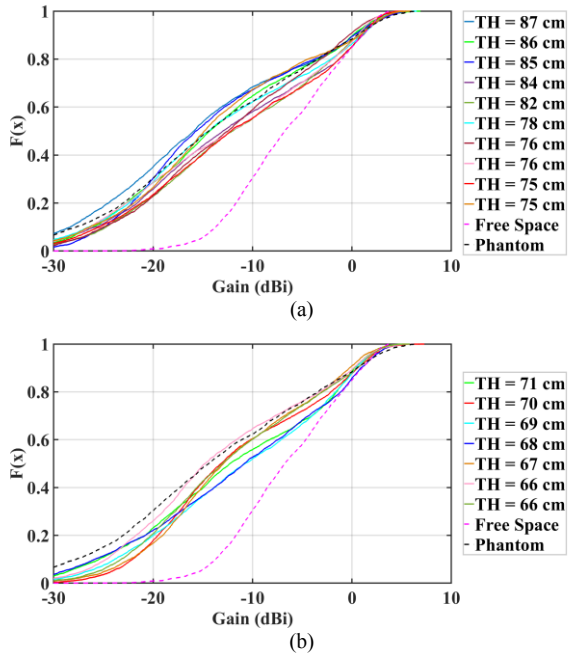

(a)

(b)

Fig. 11. The comparison of CDFs in the talk bottom edge-mounted mode for phantom and human subjects of (a) group 1, (b) group 2.

difference between samples for the top edge-mounted mode is higher than that for the bottom edge-mounted mode.

V. EFFECT OF CLOTHES ON THE BODY BLOCKAGE

The effect of the clothes on the body blockage for the body phantom has been investigated. Fig. 12 illustrates the CDFs for the phantom with a thin cotton T-shirt, thick cotton work clothes, 60/40 % polyester/ polyurethane raincoat, leather jacket, and winter jacket.

The antenna position relative to the user body is adjusted for a common data mode posture. The antenna-user distance and antenna height above the chair seat are 20 cm and 52 cm, respectively. The angle of the antenna relative to the horizon (θa) is 45˚. Within window size of 40˚, at CDF of 0.6, the maximum gain difference is 1.5 dB between naked phantom and phantom with the winter jacket. Within window sizes larger than 40˚, the CDFs of blockage patterns for different clothes get very close to each other. Fig. 13 illustrates the blockage patterns of the phantom with different types of clothes.

The effect of a thin cotton T-shirt, thick cotton work clothes, and leather jacket on the human blockage pattern with torso height of 85 cm in a similar posture is investigated as well. Fig. 14 shows the CDFs corresponding to different types of clothes. Within window sizes larger than 40˚, the CDFs of blockage patterns for different types of clothes get very close to each other.

To compare different types of clothes considering both shadowing and reflections, blockage pattern power ratio (BPPR) is presented. BPPR is the amount of the power in the blockage pattern in comparison with the power in the antenna free space pattern.

BPPR is defined as

$$BPPR = 10\log\left(\frac{\sum_{\theta_{min}}^{\theta_{max}}\sum_{\phi_{min}}^{\phi_{max}} G_{blockage\ pattern}}{\sum_{\theta_{min}}^{\theta_{max}}\sum_{\phi_{min}}^{\phi_{max}} G_{free\ space}}\right) \quad (3)$$

where, θ_{min} and θ_{max} are 10˚ and 100˚, respectively. ϕ_{min} and ϕ_{max} are defined as

$$\phi_{min} = 180° - window\ size/2$$
$$\phi_{max} = 180° + window\ size/2$$

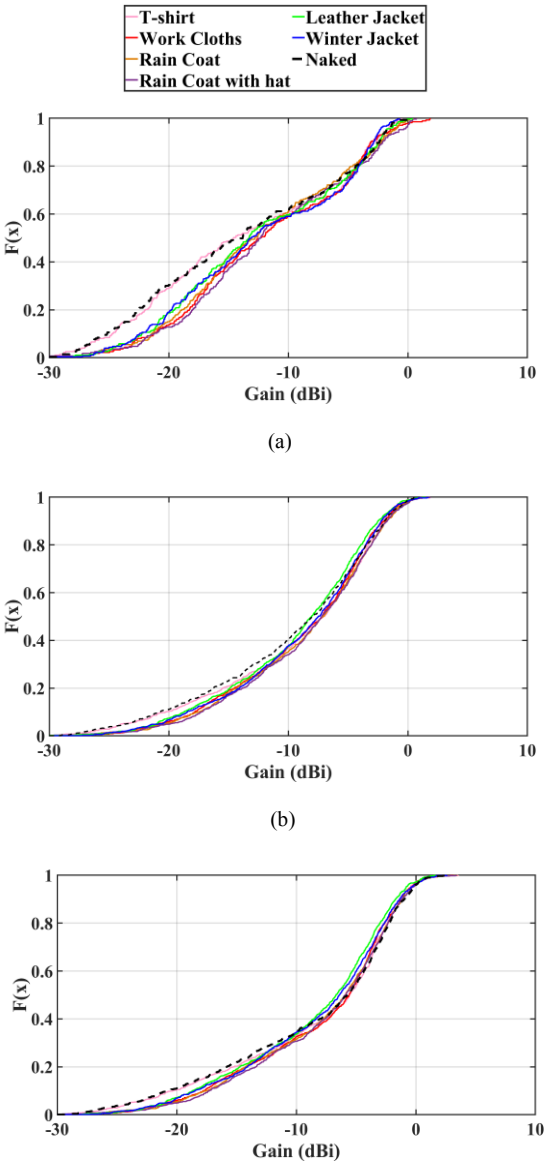

Fig. 12. The comparison of CDFs of the phantom's blockage patterns for different types of clothes within the window size of (a) 40°, (b) 80°, and (c) 140°.

Three different regions are studied, and the results are illustrated in Table III. At pure shadow region (window size of 40˚) and semi-shadow region (window size of 80˚), the blockage loss of the naked phantom is higher than that of the phantom with clothes. It can be concluded that induced surface currents on the clothes deliver more power to the area behind the body. For the window size of 140˚, the effect of the reflected and diffracted waves would be evaluated as well. It is observed that the BPPR of the phantom with the leather jacket is lower than that of the naked phantom and phantom with other types of clothes. Therefore, the reflection from the leather jacket is less than that from other clothes and the human skin. The highest BPPR is related to the raincoat with a hat for all three regions.

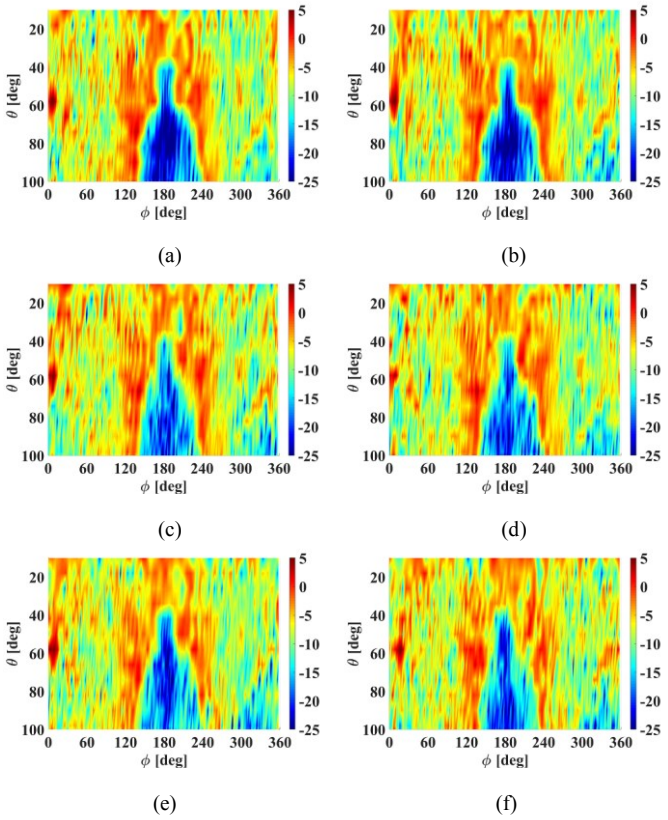

Fig. 13. The blockage patterns of the phantom (a) without clothes, and phantom with (b) T-shirt, (c) raincoat, (d) work clothes, (e) leather jacket, and (f) winter jacket.

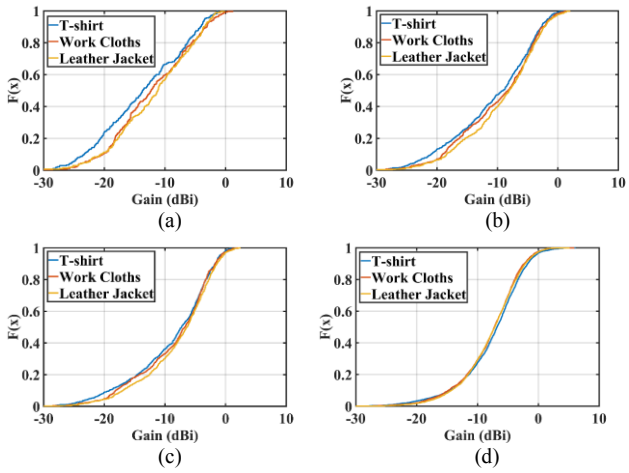

Fig. 14. The comparison of CDFs of human's blockage patterns for different types of clothes within the window size of (a) 40°, (b) 80°, (c) 140°, and (d) 360°.

VI. Blockage Assessment Using Full-body Phantom

As in optics, the relative position of the user and UE antenna determines the size of the shadow. Several measurements using full-body phantom have been conducted to study the effects of relative antenna-user distance, vertical position, and angle.

TABLE III
THE BLOCKAGE PATTERN POWER RATIO FOR DIFFERENT TYPES OF CLOTHES WITHIN DIFFERENT WINDOW SIZES.

Window Size / Type of Clothes	40˚	80˚	140˚
Naked	-15.04	-12.76	-9.45
T-shirt	-14.89	-12.7	-9.53
Raincoat	-14.42	-12.39	-9.36
Raincoat with Hat	-13.92	-12.20	-9.26
Work Clothes	-13.97	-12.41	-9.54
Leather Jacket	-14.41	-12.65	-10.12
Winter Jacket	-14.3	-12.66	-9.69

A. *Impact of the Distance*

The UE antenna is positioned at a height of 65 cm above the chair seat. The angle of the antenna to the horizon is 90˚. The blockage of the body phantom is measured for distances of 10, 20, and 30 cm from the phantom.

Fig. 16 illustrates the CDFs of the blockage patterns for different distances of the mobile phone antenna from the body phantom within different window sizes. As can be seen, by increasing the distance of the antenna from the phantom, the blockage intensity is decreased. At CDF of 0.6 within the window of 80˚, the gain difference between the distance of 10 cm with 20 cm and 30 cm is 3.4 dB and 4.2 dB, respectively. The gain difference between 20 cm and 30 cm distances is 0.8 dB. When the mobile is very close to the body, a large portion of radiated waves is blocked by the body. As the distance increases, more power will propagate around the user's body to the behind, which leads to lower body blockage. Fig. 15 illustrates a simplified 2-D blockage model [22]. In this model, the blocking object is approximated by a rectangular screen with a width of w_u and a height of h_u. The size of the antenna is very small relative to the dimension of the body and is approximated as a point source. The user's body blocks the signals coming within a blocking sector of angles (θ, φ) in space. As the distance increases, the blocking angles and the size of the blocking sector decrease. By increasing the distance, the slope of shadow size changes with respect to the antenna-user distance decreases. It is observed that the power distribution for distances of 20 cm and 30 cm are very similar.

B. *Impact of the Relative Vertical Position*

The mobile phone antenna is positioned at a distance of 15 cm from the body surface with a relative angle of 40˚ to the horizon. The impact of the mobile antenna's height relative to the chair seat is illustrated in Fig. 17. As can be seen, increasing the height decreases the body blockage intensity. By increasing the height of the antenna above the chair seat, the relative antenna-user height and the effective height of the blocking object decreases. Decreasing the height of the blocking object would decrease the height of the shadow. At CDF of 0.6, within the window of 80˚, the blockage pattern gains for heights of 30, 50, and 70 cm are –12, –8.6, and –5.4 dB, respectively.

C. *Impact of the Relative Angle*

The impact of the relative angle of the antenna to the horizon is demonstrated in Fig. 18. In this study, the mobile phone antenna is positioned at a height of 50 cm above the chair seat and a distance of 15 cm from the body phantom. It is observed that increasing the angle increases the blockage. For the gain less than –10 dB, the CDF corresponding to the angle of 10˚ is higher than that for 40˚ and 70˚. For the angle of 10˚, the main beam of the antenna is toward the top part of the torso including the head and neck. Therefore, more power can reach the behind of the

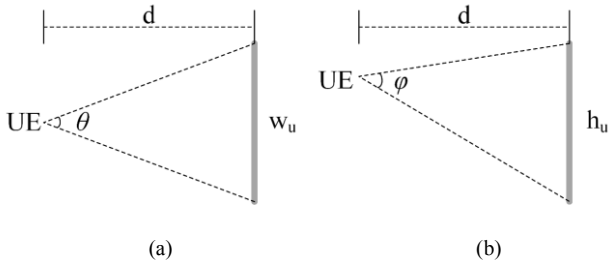

(a) (b)

Fig. 15. The user shadowing model, (a) Projection from above, (b) Projection from side.

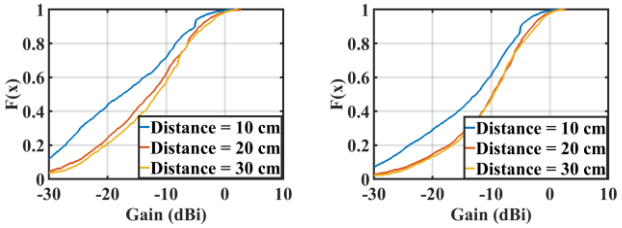

(a) (b)

Fig. 16. The comparison of CDFs of phantom blockage pattern for different relative body-antenna distances for window size of (a) 80°, (b) 140°.

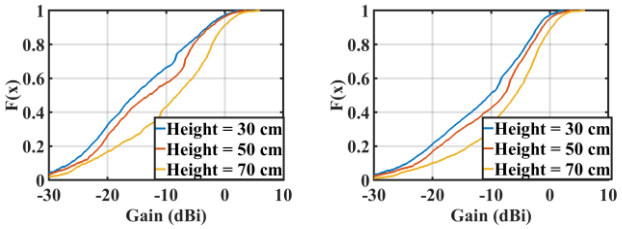

(a) (b)

Fig. 17. The comparison of CDFs of phantom blockage pattern for different heights for window size of (a) 80°, (b) 140°.

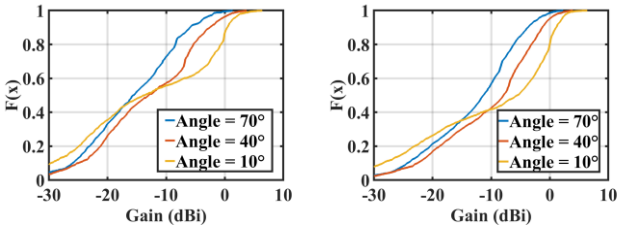

(a) (b)

Fig. 18. The comparison of CDFs of phantom blockage pattern for different relative angles to the horizon for window size of (a) 80°, (b) 140°.

body. The lower part of the torso is illuminated by low power beams of the antenna at the angle of 10˚. Therefore, compared with angles of 40˚ and 70˚, the power strength is lower in the shadow region. At CDF of 0.6, within the window of 80˚, the blockage pattern gains are –12.5, –8.6, and –6.7 dB, for relative angles of 70˚, 40˚, and 10˚, respectively.

VII. Conclusion

In this paper, the blockage pattern of full-body phantom has been compared with 17 human subjects in data and talk modes. In the data mode, the phantom's blockage pattern in the shadow region is highly correlated with human subjects having a height close to the height of the phantom. The blockage power distributions of the phantom and subjects in group 1 are very similar. For group 2, the blockage of the phantom is larger than that of human subjects within all window sizes.

In the talk mode, the blockage pattern of the phantom is highly correlated with the blockage pattern of human subjects for both top and bottom edge-mounted modes.

At pure shadow region (window size of 40˚) and semi-shadow region (window size of 80˚), the blockage loss of the naked phantom is higher than that of the phantom with clothes. In the antenna coverage area (window size of 140˚), the BPPR of the phantom with the leather jacket is lower than that of the naked phantom and phantom with other types of clothes. The highest BPPR is related to the raincoat with a hat for all three regions.

Acknowledgment

The authors would like to thank the SPEAG (Zurich, Switzerland) for providing the full-body phantom for body blockage measurements.

References

[1] J. G. Andrews, S. Buzzi, W. Choi, S.V. Hanly, A. Lozano, A.C. Soong, and J.C. Zhang, "What will 5G be?," *IEEE J. Sel. Areas Commun.*, vol. 32, no. 6, pp. 1065–1082, Jun. 2014.

[2] T. S. Rappaport, S. Sun, R. Mayzus, H. Zhao, Y. Azar, K. Wang, G.N. Wong, J.K. Schulz, M. Samimi, and F. Gutierrez, "Millimeter wave mobile communications for 5G cellular: It will work!," *IEEE Access,* vol. 1, pp. 335–349, May 2013.

[3] I. A. Hemadeh, K. Satyanarayana, M. El-Hajjar, and L. Hanzo, "Millimeter-wave communications: Physical channel models, design considerations, antenna constructions, and link-budget," *IEEE Commun. Surveys Tuts.*, vol. 20, no. 2, pp. 870–913, Dec. 2017.

[4] W. Roh, J.Y. Seol, J. Park, B. Lee, J. Lee, Y. Kim, J. Cho, K. Cheun, and F. Aryanfar, "Millimeter-wave beamforming as an enabling technology for 5G cellular communications: Theoretical feasibility and prototype results," *IEEE Commun. Mag.,* vol. 52, no. 2, pp. 106-113, Feb. 2014.

[5] W. Hong, K. H. Baek, and S. Ko, "Millimeter-wave 5G antennas for smartphones: Overview and experimental demonstration," *IEEE Trans. Antennas Propag.*, vol. 65, no. 12, pp. 6250–6261, Dec. 2017.

[6] Y. Li and K. M. Luk, "A multibeam end-fire magnetoelectric dipole antenna array for millimeter-wave applications," *IEEE Trans. Antennas Propag.*, vol. 64, no. 7, pp. 2894–2904, Jul. 2016.

[7] M. F. Khajeim, G. Moradi, R. S. Shirazi, S. Zhang, and G. F. Pedersen, "Wideband vertically polarized antenna with endfire radiation for 5G mobile phone applications," *IEEE Antennas Wireless Propag. Lett.,* vol. 19, no. 11, pp. 1948–1952, Nov. 2020.

[8] 3GPP TR 38.901 V14.3.0 (2017-12), "Technical Specification Group Radio Access Network; Study on Channel Model for Frequencies from 0.5 to 100 GHz (Rel. 14)," Dec. 2017.

[9] METIS 2020, "METIS channel model, Deliverable D1.4v3," Jul. 2015.

[10] V. Raghavan, L. Akhoondzadeh-Asl, V. Podshivalov, J. Hulten, M.A. Tassoudji, O.H. Koymen, A. Sampath, and J. Li, "Statistical blockage modeling and robustness of beamforming in millimeter-wave systems," *IEEE Trans. Mic. Theory Techniq*., vol. 67, no. 7, pp. 3010–3024, Jul. 2019.

[11] P. Liu, I. Syrytsin, J.Ø. Nielsen, G. F. Pedersen, and S. Zhang, "Characterization and modeling of the user blockage for 5G handset antennas," *IEEE Trans. Instrumentation Measurement,* vol.70, pp. 1–11, Nov. 2020.

[12] M. Peter, M. Wisotzki, M. Raceala-Motoc, W. Keusgen, R. Felbecker, M. Jacob, S. Priebe, and T. Kürner, "Analyzing human body shadowing at 60 GHz: Systematic wideband MIMO measurements and modeling approaches," in *Proc. 6th European Conf. Ant. Propagat. (EUCAP),* Prague, Czech Republic, Mar. 2012, pp. 468–472.

[13] I. Syrytsin, S. Zhang, G. F. Pedersen, and Z. Ying, "User effects on the circular polarization of 5G mobile terminal antennas," *IEEE Trans. Antennas Propag.*, vol. 66, no. 9, pp. 4906–4911, Jun. 2018.

[14] I. Syrytsin, S. Zhang, G. F. Pedersen, and A. S. Morris, "User-shadowing suppression for 5G mm-wave mobile terminal antennas," *IEEE Trans. Antennas Propag.*, vol. 67, no. 6, pp. 4162-4172, Mar. 2019.

[15] I. Syrytsin, S. Zhang, G. F. Pedersen, K. Zhao, T. Bolin, and Z. Ying, "Statistical investigation of the user effects on mobile terminal antennas for 5G applications," *IEEE Trans. Antennas Propag.*, vol. 65, no. 12, pp. 6596-6605, Mar. 2017.

[16] K. Zhao, J. Helander, D. Sjöberg, S. He, T. Bolin, and Z. Ying, "User body effect on phased array in user equipment for the 5G mmWave communication system," *IEEE Antennas Wireless Propag. Lett.,* vol. 16, pp. 864–867, Sep. 2016.

[17] TS38.101-2 v15.0.0 User Equipment (UE) radio transmission and reception; Part 2: Range 2 Standalone (Release 15), Jun. 2018.

[18] mmW-POPEYE10, https://speag.swiss/products/em-phantoms/phantoms-3/popeye-v10-3/

[19] I. Syrytsin, S. Zhang, G. F. Pedersen, and A. S. Morris, "Compact quad-mode planar phased array with wideband for 5G mobile terminals," *IEEE Trans. Antennas Propag.,* vol. 66, no. 9, pp. 4648-4657, May 2018.

[20] J. O. Nielsen, G. F. Pedersen, K. Olesen, and I. Z. Kovacs, "Statistics of measured body loss for mobile phones," *IEEE Trans. Antennas Propag.*, vol. 49, no. 9, pp. 1351–1353, Sep. 2001.

[21] W. H. Press, S. A. Teukolsky, W. T. Vetterling, and B. P. Flannery, "Numerical Recipes in C," in *Statistical Description of Data,* 2nd ed., Cambridge university press, 1988, pp. 636–638.

[22] T. Bai, and R.W. Heath, "Analysis of self-body blocking effects in millimeter wave cellular networks," in *Proc. 48th Asilomar Conf. Signals, Systems and Computers,* Pacific Grove, CA, USA, Nov. 2014, pp. 1921–1925.